Global Gene Expression Analysis of Reactive Stroma in Prostate Cancer

Olga Dakhova,[1,4] Mustafa Ozen,[1,4] Chad J. Creighton,[2] Rile Li,[1] Gustavo Ayala,[1] David Rowley,[3] and Michael Ittmann[1,4]

Abstract

Purpose: Marked reactive stroma formation, designated as grade 3 reactive stroma, is associated with poor outcome in clinically localized prostate cancer. To understand the biological processes and signaling mechanisms underlying the formation of such reactive stroma, we carried out microarray gene expression analysis of laser-captured reactive stroma and matched normal stroma.

Experimental Design: Seventeen cases of reactive stroma grade 3 cancer were used to laser-capture tumor and normal stroma. Expression analysis was carried out using Agilent 44K arrays. Up-regulation of selected genes was confirmed by quantitative reverse transcription-PCR. Expression data was analyzed to identify significantly up- and down-regulated genes, and gene ontology analysis was used to define pathways altered in reactive stroma.

Results: A total of 544 unique genes were significantly higher in the reactive stroma and 606 unique genes were lower. Gene ontology analysis revealed significant alterations in a number of novel processes in prostate cancer reactive stroma, including neurogenesis, axonogenesis, and the DNA damage/repair pathways, as well as evidence of increases in stem cells in prostate cancer reactive stroma.

Conclusions: Formation of reactive stroma in prostate cancer is a dynamic process characterized by significant alterations in growth factor and signal transduction pathways and formation of new structures, including nerves and axons.

Prostate cancer remains the most common malignancy affecting men and the third leading cause of cancer-related death of men in the United States. It has been appreciated for many years that the tumor microenvironment plays an important role in the initiation and progression of prostate and other cancers (1–3). The tissues surrounding the cancer cells in prostate cancer are distinct from the normal mesenchymal tissues of the prostate and consist of a mixture of fibroblasts, myofibroblasts, endothelial cells, immune cells, other cells, and altered extracellular matrix. We have previously shown an increase in prostate cancer stroma of cells with a myofibroblastic phenotype (4) that synthesize collagen I (4) and expressed tenascin, which is shown to be involved in modulation of cell growth and tumorigenesis. Using *in vitro* models, we showed that transforming growth factor (TGF) β1 enhances the transformation of prostatic fibroblasts into the myofibroblastic phenotype (4). Other key processes previously identified in prostate cancer stroma include angiogenesis (5), as well as infiltration of immune cells (3).

We recently examined the clinical implications of the histologic variability of reactive stroma in prostate cancer (6, 7). Whereas some prostate cancers have little histologic alteration of the surrounding stroma compared with normal stroma in benign prostate, a subset of cancers reveals an obvious alteration in the surrounding stroma. Of note, we have shown men with tumors having the most profound histologic alterations of reactive stroma, which is termed grade 3 reactive stroma, had reduced biochemical recurrence-free survival in tissue microarray (6) and biopsy studies (7). This predictive ability was independent of Gleason score and other pathologic variables.

To understand the mechanisms by which reactive stroma can influence tumor behavior, we examined global changes in gene expression in grade 3 reactive stroma relative to paired benign prostatic stroma using expression microarray analysis on laser-captured RNAs from these two tissue types. By focusing on grade 3 reactive stroma, which is associated with prostate cancer progression, we hope to indentify key changes in prostate reactive stroma that are associated with aggressive prostate cancer. Our analysis has revealed significant alterations in a number of novel

Authors' Affiliations: Departments of [1]Pathology, [2]Medicine, and [3]Molecular and Cellular Biology, Baylor College of Medicine; and [4]Michael E. DeBakey Veterans Affairs Medical Center, Houston, Texas

Received 7/23/08; revised 2/25/09; accepted 3/23/09; published OnlineFirst 6/9/09.

Grant support: National Cancer Institute to the Tumor Microenvironment Network (1U54CA126568; D. Rowley), the P30 Cancer Center support grant (P30 CA125123), the Baylor Prostate Cancer SPORE (P50CA058204), the Department of Veterans Affairs Merit Review program (M. Ittmann), the Diana Helis Henry Medical Research Foundation (M. Ittmann, G. Ayala, D. Rowley), and by the use of the facilities of the Michael E. DeBakey Veterans Affairs Medical Center.

The costs of publication of this article were defrayed in part by the payment of page charges. This article must therefore be hereby marked *advertisement* in accordance with 18 U.S.C. Section 1734 solely to indicate this fact.

Note: Supplementary data for this article are available at Clinical Cancer Research Online (http://clincancerres.aacrjournals.org/).

Current address for M. Ozen: Department of Medical Genetics, Yeditepe Medical School, Istanbul, Turkey.

Requests for reprints: Michael Ittmann, Department of Pathology, Baylor College of Medicine, One Baylor Plaza, Houston, TX 77030. Phone: 713-798-6196; Fax: 713-798-5838; E-mail: mittmann@bcm.tmc.edu.

doi:10.1158/1078-0432.CCR-08-1899

Translational Relevance

The tumor microenvironment can influence cancer progression in a variety of malignancies. In prostate cancer, a marked stromal response is associated with poor outcome independent of Gleason score and other pathologic variables. In this study, we use microarray gene expression analysis to define key processes and signaling pathways associated with the formation of prostate cancer reactive stroma. Future studies may identify individual biomarkers within the reactive stroma that are associated with prostate cancer progression. Furthermore, we have identified a number of growth factor and signal transduction pathways that are potential drug targets in reactive stroma.

pathways not previously identified in prostate cancer reactive stroma, including neurogenesis, axonogenesis, and the DNA damage/repair pathways, as well as evidence of a possible increase in stem cells in prostate cancer reactive stroma.

Materials and Methods

Laser-capture microdissection of stromal tissues. Laser-capture microdissection was done using HistoGene LCM Frozen Section Staining Kit (Molecular Devices). Briefly, 10-μm-thick frozen sections were cut from tissue cores of normal and cancerous area of fresh unfixed prostatectomy specimen. All cancer tissues were from cases with grade 3 reactive stroma as identified on paraffin-embedded whole-mount sections, and frozen sections were confirmed to have grade 3 reactive stroma by a pathologist with experience in stromal grading (Gustavo Ayala (GA)) before laser capture. Reactive stroma is less eosinophilic than normal stroma because of loss of smooth muscle, and there is deposition of collagen fibrils and extracellular matrix. Reactive stroma has a higher cellularity than normal stroma because of increased fibroblasts and myofibroblasts. The cells, which now resemble fibroblasts more than muscle cells, are characteristically disordered and show irregular length and thickness. A characteristic of reactive stroma is that these cells are arranged in an irregular fascicular pattern in a delicate fibrillary background. Grade 3 reactive stroma has at least 51% reactive stroma in the tumor section, as described previously (7). Frozen sections were placed on noncharged glass slides and stored at -80°C before use. Slides were stained and dehydrated according the manufacturer protocol. Laser-capture microdissection was done using a Pixcell II laser-capture microdissection microscope (Molecular Devices), using a 15-μm laser spot size, 0.75- to 0.90-ms laser pulse, and 45-mV beam power. Approximately 4,000 to 8,000 laser pulses of stroma between the glands in normal and prostate cancer tissues were captured on 2 to 3 caps (1,500-2,500 spots).

Amplification and expression microarray analysis. Total RNA was extracted from laser-capture microdissection–captured stroma using PicoPure RNA Isolation Kit (Molecular Devices) according to the manufacturer's protocol. It was then amplified using RiboAmp RNA Amplification Kit (Molecular Devices). Two rounds of *in vitro* amplification were done according to the manufacturer's protocol. The quantity of amplified RNA was measured by spectrophotometer at optical density (OD) 260 nm. Different starting amounts of control RNA were used to confirm linear RNA amplification. The cDNA reverse transcription and fluorescent labeling reactions were carried out using Invitrogen SuperScript Plus Direct cDNA Labeling System with Alexa Fluor 5′-Aminohexylacrylamido-dUTP (Invitrogen). Briefly, 2.5 μg of aRNA and Universal Human Reference RNA (Stratagene) were labeled in reverse transcription with Alexa647 and Alexa555 aha-dUTPs, respectively. After labeling, 2.5 μg of each aRNA was mixed with 2.5 μg of reference RNA and purified with SuperScript Plus Direct cDNA Labeling System purification module according to manufacturer's instructions. Eluted sample was mixed with 10× Blocking Solution and 2× HiRPM buffer (Agilent Technologies), incubated for 2 min at 95°C to 98°C and hybridized on 4 × 44K Whole Human Genome Oligo Microarray chip (Agilent Technologies) using SureHyb DNA Microarray Hybridization Chambers in DNA Microarray hybridization oven (Agilent Technologies) at 10 rpm, 65°C for 20 h. After hybridization, slides were washed in Gene Expression Wash Buffer 1 and 2 for 1 min and then dried by centrifugation at 2,000 rpm for 2 min. Microarrays were scanned with a dynamic autofocus microarray scanner (Agilent Microarray Scanner–G2565BA, Agilent Technologies) using Agilent-provided parameters (Red and Green photomultiplier tube (PMT) were each set at 100%, and scan resolution was set to 5 μm). The Feature Extraction Software v9.1.3.1 (Agilent Technologies) was used to extract and analyze the signals. To validate the amplification process, amplified and unamplified RNAs were labeled and hybridized to an Agilent 21K oligonucleotide array.

Statistical analysis microarray expression data. Expression arrays were processed and loess normalized using BioConductor (8). Array data has been deposited in the public Gene Expression Omnibus database, accession GSE11682. Arrays were processed in batches at different times (with an equal number of cancer and normal samples in each batch); to correct for batch effects, the estimated expression values within each batch were transformed to SDs from the mean [the results when using this method being very similar to what was observed using the alternative "Combat" algorithm (ref. 9)]. Two-sided *t* tests determined significant differences in mean gene mRNA levels between groups. False discovery rate was estimated by the method of Storey and Tibshirani (10) and by 100 permutations of the profile group labels. Expression values were visualized as color maps using the Cluster (11) and Java TreeView (12) software. Gene ontology annotation terms were searched within gene sets essentially, as described previously (13). Protein interaction network analysis was carried out essentially, as described previously (14). The entire set of protein-protein interactions cataloged in the Human Protein Reference Database[5] was obtained in September 2007. Interactions involving the same gene product interacting with itself were excluded from the analysis. Graphical visualization of the interaction network was generated using the Cytoscape software (15).

Quantitative reverse transcription-PCR (RT-PCR). Real-time PCR was carried out in sealed 96-well microtiter plates (Bio-Rad) with Absolute Blue QPCR SYBR Green Fluorescein Mix (Thermo Fisher Scientific, Inc.) and Bio-Rad I-cycler QPCR Machine (Bio-Rad). All 17 tumor and normal stromal RNAs were analyzed in triplicate. Primers used are summarized in Supplementary Table S1. The PCR conditions were 20-s denaturation, 30-s annealing at the optimal temperature of the primer, and 30-s extension at 72°C for 40 cycles. cDNA from Universal Human Reference RNA (Stratagene), which was serially diluted from 1:5 to 1:10,000, was used to generate standard curves. The relative copy number of transcript for each gene was normalized by transcript level of the housekeeping gene (*HPRT1*) in each sample. Each PCR experiment was carried out in triplicate. Student *t* test was done to validate statistically significant differences. Data with $P < 0.05$ in normal versus reactive stroma comparison were considered significant.

Immunohistochemistry. Immunohistochemistry was done on a small-tissue microarrays with 10 reactive stroma grade 3 cancers and matched normal tissues essentially, as described previously (16). For extracellular signal-regulated kinase 1 immunohistochemistry, antigen retrieval was carried out with 0.1 mol/L Tris (pH 9.0) for 25 min with steam heat. Anti–extracellular signal-regulated kinase 1 antibody (Cat 32537; Abcam) was used at 1:500 dilution for 30 min at room temperature. For anti–GSK-3β immunohistochemistry, antigen retrieval

[5] www.hprd.org

was done in10 mmol/L citrate buffer (pH 6.0) for 20 min in steam heat. Anti–GSK-3β antibody (Cat 9332; Cell Signaling Technology) was used at 1:60 dilution overnight at 4°C. Antigen retrieval for c-KIT immunohistochemistry was done in Reveal Decloaker Buffer (Biocare Medical) in a pressure cooker for 10 min. Anti–c-Kit antibody (Cat A4502; Dako) was used at 1:100 dilution for 30 min at room temperature.

Analysis of breast stroma microarray expression data. We obtained the expression profile data set from Finak et al. (17) of breast cancer stroma and normal stroma (Gene Expression Omnibus accession GSE9014; dye-swap profiles not used); for duplicate profiles, log-transformed ratios were averaged. Log ratios of each profile were scale normalized across the ~45 K transcript probes to median value of zero. Sample E1527 seemed an obvious outlier and so was removed from the analysis. Mapping between the prostate and breast stroma profile data sets was done using the Agilent transcript probe identifier. For heat map representation of the breast stroma data, the expression values for each gene were centered on the mean centroid between the normal and cancer groups. For each sample, the mean centroid was first defined without the given sample; the genes in the left out profile were then centered on this mean centroid (in this way, when using the average values to classify cancer from normal in Fig. 4, the labeling of the classified sample itself played no role in the prediction).

Results

Laser-capture microdissection and expression array analysis of grade 3 reactive stroma in prostate cancer. To evaluate global gene expression changes in grade 3 reactive stroma versus normal peripheral zone stroma, we did laser-capture microdissection and expression array analysis of stroma from 17 grade 3 reactive stroma prostate cancer tissues and matched normal peripheral zone tissues. Captured RNAs were amplified and hybridized to Agilent 60-mer oligonucleotide 4 × 44K Whole Human Genome expression microarrays, which represent ~41,000 unique genes and transcripts. To confirm that our amplification protocol is not introducing significant bias, we amplified a prostate cancer RNA and then labeled and hybridized the RNA to a 21K oligonucleotide array and compared the expression results with unamplified RNA (Fig. 1A). After normalization and filtering for the signals with low intensity, 88.7% of the genes showed no >1.5-fold difference. In another way of comparison, only 3.04% (140 of 4,602) of the genes changed their expression levels by ≥2-fold after amplification, similar to the results of other groups (18) Of note, none of the 140 genes showed a reversal of relative expression, that is, increased to decreased. In all cases, the difference was based on fold change in the same direction, that is, 3-fold versus 6-fold. Thus, although there may be some variation introduced by amplification, this is unlikely to significantly affect our overall analysis.

To assess the purity of the captured stromal RNAs, we carried out quantitative RT-PCR for prostate-specific antigen (PSA) and keratin-18, two epithelial markers expressed in normal epithelium and prostate cancer, indicating that some epithelial contamination of the stroma was present. Both were barely detectable. We were concerned that the intimate admixture of cancer epithelial cells and stroma might lead to increased contamination with epithelial cells in the cancer stroma samples when compared with normal stroma. However, there was no significant difference in the mean PSA and keratin-18 mRNA levels between cancer stroma and normal stroma RNAs ($P < 0.96$ PSA and $P < 0.26$ keratin 18; t test). When compared with prostate cancer tissue, expression of PSA was >1,600-fold higher in the tissue compared with the stroma samples (Fig. 1B), indicating that there was minimal epithelial contamination of the laser-captured stromal tissues.

We next analyzed the expression of ~19,075 genes giving detectable signals in the 17 grade 3 stroma RNAs and matched normal peripheral zone stromal samples using expression microarrays (Fig. 2A). A total of 1,675 probes representing 1,141 unique genes were differentially expressed at $P < 0.01$; 544 unique genes were higher in the reactive stroma, and 606 unique genes were lower (9 genes in the 544 set were represented in the 606 set by different probes). The 1,675

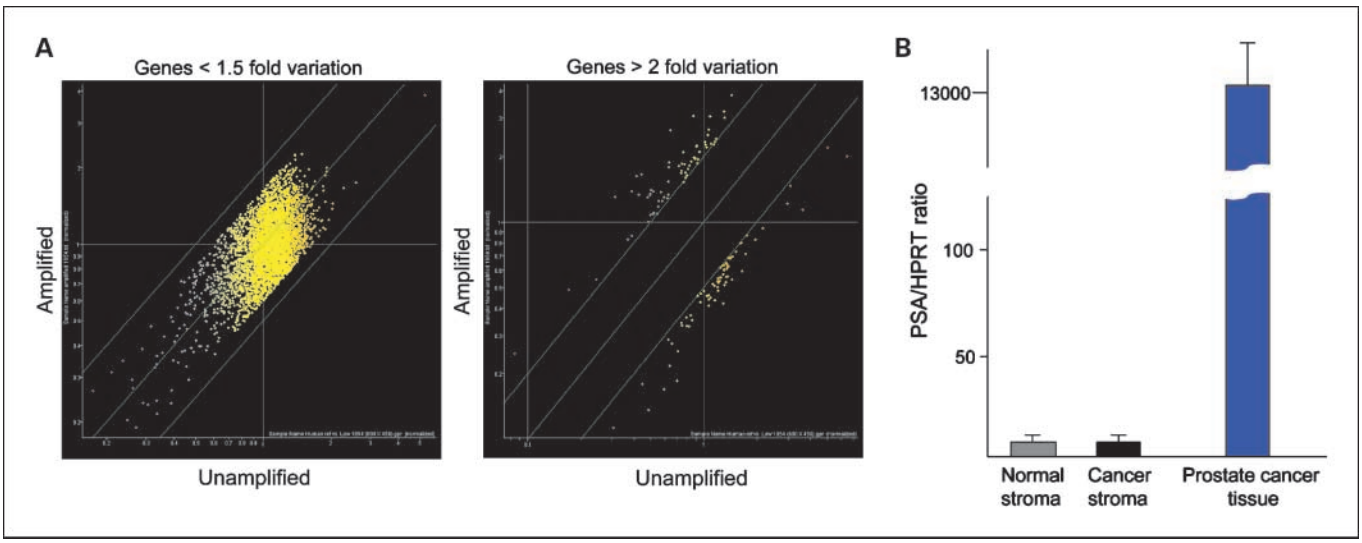

Fig. 1. Validation of RNA amplification and laser capture. *A,* genes with ≤1.5-fold variation between amplified and unamplified RNA; 88.7% of genes met this criteria (*left*); genes with >2-fold variation between amplified and unamplified RNAs (*right*), which constitute only 3% of the total. *B,* quantitative RT-PCR of PSA expression in laser-captured normal and tumor stroma and prostate cancer tissue. PSA content of normal and tumor stroma was not significantly different, and both were 1,600-fold less than undissected prostate cancer tissue. Mean ± SD of triplicate determinations is shown. PSA copy number was normalized to HPRT copy number relative to the universal reference RNA.

significant probes significantly exceed the number of probes that would be expected to be differentially expressed by chance alone at this *P* value (~450 probes by probability calculation, 382 by permutation testing). Thus, there are significant differences in gene expression between grade 3 reactive stroma and normal prostate stroma. One obvious histologic and immunohistochemical characteristic of grade 3 reactive stroma is the decreased amounts of differentiated smooth muscle in

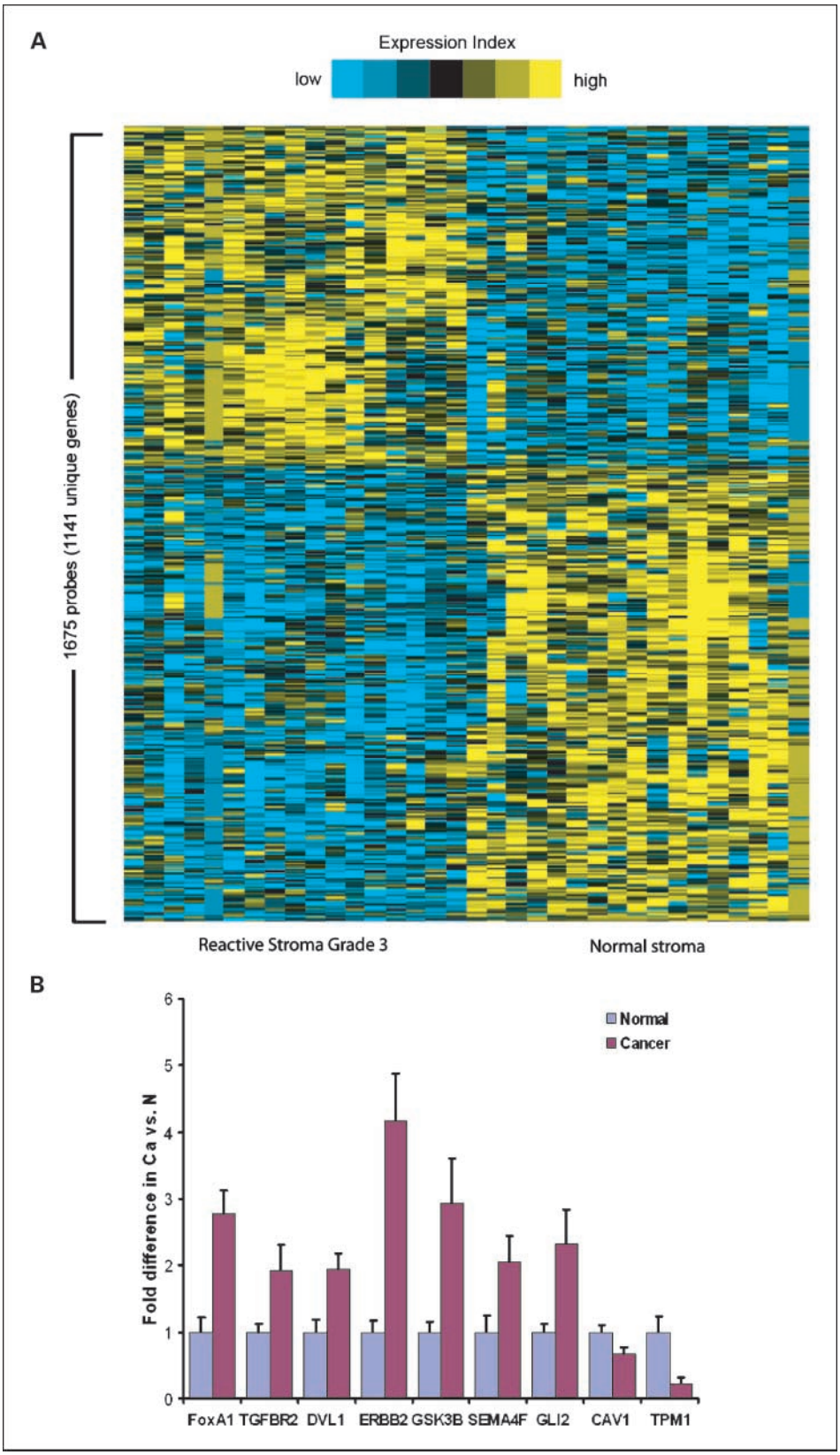

Fig. 2. A gene transcription signature of grade 3 reactive stroma in prostate cancer. *A,* heat map representation of 1,675 gene probes (1,141 unique named genes) differentially expressed ($P < 0.01$) in reactive prostate stroma compared with normal stroma (*rows*, genes; *columns*, profiled samples; *yellow*, high expression). *B,* quantitative RT-PCR validation of selected genes from the list of 1,141 ($P < 0.05$ for each; *t* test). Mean ± SD of triplicate determinations. HPRT was used for copy number normalization.

Table 1. Significantly enriched gene ontology terms ($P < 0.01$) for genes up-regulated ($P < 0.01$) in reactive stroma

Category/term	P	Fold
Neurogenesis		
Dendrite development	0.0003	11.7
Neurite development	0.0024	10.5
Neural crest cell migration	0.0081	7
Axonogenesis	0.0008	5.4
Synapse organization and biogenesis	0.0023	5.3
Neurite morphogenesis	0.0013	4.9
Cell soma	0.0088	4.8
Synaptic transmission	0.0096	2.2
DNA damage and repair		
DNA damage checkpoint	0.0068	5.2
DNA damage response, signal transduction	0.0015	4.8
DNA integrity checkpoint	0.0100	4.7
Response to DNA damage stimulus	0.0058	2
Morphogenesis and development		
Cell part morphogenesis	0.0013	4.9
Cell projection morphogenesis	0.0013	4.9
Cell projection organization and biogenesis	0.0021	4.5
Epidermis development	0.0025	3.4
Cellular structure morphogenesis	0.0015	3.1
Metabolic processes		
Cellular polysaccharide catabolic process	0.0053	8.1
Polysaccharide catabolic process	0.0053	8.1
Oxidoreductase activity, acting on CH-OH group of donors	0.0098	2.7
Monocarboxylic acid metabolic process	0.0009	2.5
Fatty acid metabolic process	0.0045	2.5
Regulation of hydrolase activity	0.0063	2.4
Kinase activity		
Calmodulin-regulated protein kinase activity	0.0098	6.6
Protein kinase cascade	0.0035	2.6
Protein serine/threonine kinase activity	0.0016	2
Membrane and ion transport		
Chloride transport	0.0080	4
Porter activity	0.0089	2.2
Electrochemical potential–driven transporter activity	0.0092	2.2
Carrier activity	0.0053	2
Transcription regulation		
Positive regulation of transcription from RNA pol II promoter	0.0051	2.6
Apoptosis		
DNA fragmentation during apoptosis	0.0066	7.5
Cell structure disassembly during apoptosis	0.0018	7.4

reactive stroma (Supplementary Fig. S1). Consistent with this, we noted that tropomyosins (multiple probes of each) and caveolin-1 (multiple probes), which are characteristically expressed in differentiated smooth muscle, were all significantly down-regulated in Grade 3 reactive stroma.

Validation of expression microarray results by quantitative RT-PCR. To validate the results of our expression microarrays, we next carried out quantitative RT-PCR analysis of the RNAs used in the expression microarray studies. We analyzed a total of seven genes that were up-regulated in cancer stroma (*FOXA1*, *TGFBR2*, *DVL1*, *ERBB2*, *GSK3B*, *SEMA4F*, and *GLI2*) and two that were down-regulated (*CAV1* and *TPM1*). As shown in Fig. 2B, in all cases, we were able to confirm statistically significant up- or down-regulation ($P < 0.05$; t test), as predicted from the microarrays, validating the accuracy of our microarray expression data.

Gene ontology analysis of expression microarray data. To develop an objective analysis of key processes altered in the grade 3 reactive stroma, we carried out gene ontology analysis of the 1,141 genes that were significantly altered. Analysis of the 544 unique genes high in reactive stroma revealed a total 66 gene ontology annotation terms that were enriched ($P < 0.01$; one-sided Fisher's exact test) in this gene list in comparison with all the genes on the array, and of these, 46 were represented by at least 10 genes on the array. All 2,309 gene ontology terms representing at least 10 genes on the array were considered, and a number of these gene ontology terms could conceivably have been nominally significant by multiple testing. Nevertheless, simulation testing using 1,000 random gene sets yielded on average only about one fourth the number of enriched gene ontology terms ($P < 0.01$) that were observed with the actual gene set (Supplementary Fig. 2), indicating that the genes are involved in specific processes and not random. To

Table 2. Significantly up-regulated ($P < 0.01$) gene ontology terms for genes down-regulated in reactive stroma

Category/term	P	Fold
Oxygen transport		
Hemoglobin complex	0.0044	8.6
Superoxide metabolic process	0.0003	8.3
Gas transport	0.0089	6.8
Oxygen transporter activity	0.0089	6.8
Oxygen transport	0.0089	6.8
Oxygen binding	0.0067	4.1
Cytoskeleton		
Actin filament bundle	0.0014	7.9
Stress fiber	0.0014	7.9
Perinuclear region of cytoplasm	0.0012	4.2
Cytoskeleton	0.0002	2
Muscle		
Structural constituent of muscle	0.0002	5.5
Regulation of heart contraction	0.0103	3.8
Contractile fiber part	0.0092	3.3
Ion channel activity		
Channel inhibitor activity	0.0044	8.6
Ion channel inhibitor activity	0.0044	8.6
Protein folding		
Unfolded protein response	0.0044	8.6
Response to protein stimulus	0.0019	3.9
Response to unfolded protein	0.0019	3.9
Developmental processes		
Ureteric bud development	0.0006	9.7
Positive regulation of developmental process	0.0078	3.4
Regulation of developmental process	0.0043	2.2
Neurogenesis		
Positive regulation of axonogenesis	0.0057	7.9
Positive regulation of neurogenesis	0.0089	6.8
Immune system		
Leukocyte activation	0.0049	2.5
Cell activation	0.0057	2.3
Behavior		
Learning	0.0017	7.4
Locomotory behavior	0.0055	2.2
Cell motility		
Cell motility	0.0010	2.1
Cell membrane		
Lipid raft	0.0099	4.7
Others		
Histone binding	0.0001	11.2
Endopasmic reticulum-nuclear signaling pathway	0.0089	6.8
Golgi trans face	0.0039	6
Copper ion binding	0.0021	3.9

further increase the stringency, only gene ontology terms that were at least 2-fold enriched relative to all genes were considered, leaving 33 gene ontology terms. These are shown in Table 1, grouped functionally, and component genes are shown in Supplementary Table S2. Some of these gene class associations, as represented by gene ontology terms, are as would be predicted, whereas others are unexpected. The largest and most interesting is the eight neural-related gene ontology terms. These primarily relate to neurogenesis, axonogenesis, synaptogenesis, and neural biogenesis. This large cluster of gene ontology terms indicates that active neurogenesis and axonogenesis is occurring in grade 3 reactive stroma. Whereas angiogenesis is a well-known biological process in tumors, the role of axonogenesis and neurogenesis in cancer stroma is relatively unexplored. Another surprising cluster was a set of four gene ontology terms related to DNA damage checkpoint response. This finding implies that some factor in the overall tumor microenvironment, perhaps increased reactive oxygen species, is leading to DNA damage in tumor stromal cells. Genomic lesions have been reported in tumor stroma (19), which is consistent with increased DNA damage in the tumor microenvironment. Other enriched terms such as development and morphogenesis (five terms), metabolic processes (six terms), membrane and ion transport (four terms), and positive regulation of RNA polymerase II (one term) would be expected in a metabolically activated tissue compartment undergoing rapid remodeling and formation of new structures such as nerves and blood vessels. Kinase activity was also well represented (three terms), consistent with the regulatory role of kinases in cell activation. Two apoptosis terms are also identified, indicating active cell death, perhaps as a result of DNA damage or as part of a morphogenic process, is increased in reactive stroma.

A similar analysis revealed 33 gene ontology terms enriched with at least 10 genes on the array enriched at least 2-fold and $P < 0.01$ for the genes decreased in reactive stroma (Table 2 and Supplementary Table S3). Terms related to muscle cells (three terms) and cytoskeleton structure (four terms) were prominent, consistent with displacement of smooth muscle by reactive stroma, as noted above. Also of interest is a group of six gene ontology terms related to oxygen transport and superoxide metabolism. Two neurogenesis-related terms were also identified, indicating that neurogenesis is a regulated process within the reactive stroma, as would be expected in a nontransformed tissue compartment.

Protein interaction networks involving reactive stroma genes. We queried the Human Protein Reference Database catalog of >35,000 known physical protein-protein interactions (20) to determine how the reactive stroma–associated genes relate to each other in terms of interactions between their associated proteins. In the set of 1,141 genes differentially expressed in reactive compared with normal stroma, 292 Human Protein Reference Database interactions were represented (both members being included in the 1,141 gene set). Randomly selected gene sets yielded 124 interactions on average (SD = 23; Fig. 3A), indicating that many of the 292 interactions are actually involved within the reactive stroma. The 292 interactions were visualized as a graphical network (Fig. 3B). A view of the central node is shown in Fig. 3C. Of note is the prominence of signal transduction molecules in this network (*STAT1*, *STATIP1*, *LCK*, *MA2K11P1*, *PTPRF*, *MAPK3*, *PRKCD*, *PRKCA*, *HRAS*, *PLA2G4A* etc) This finding indicates

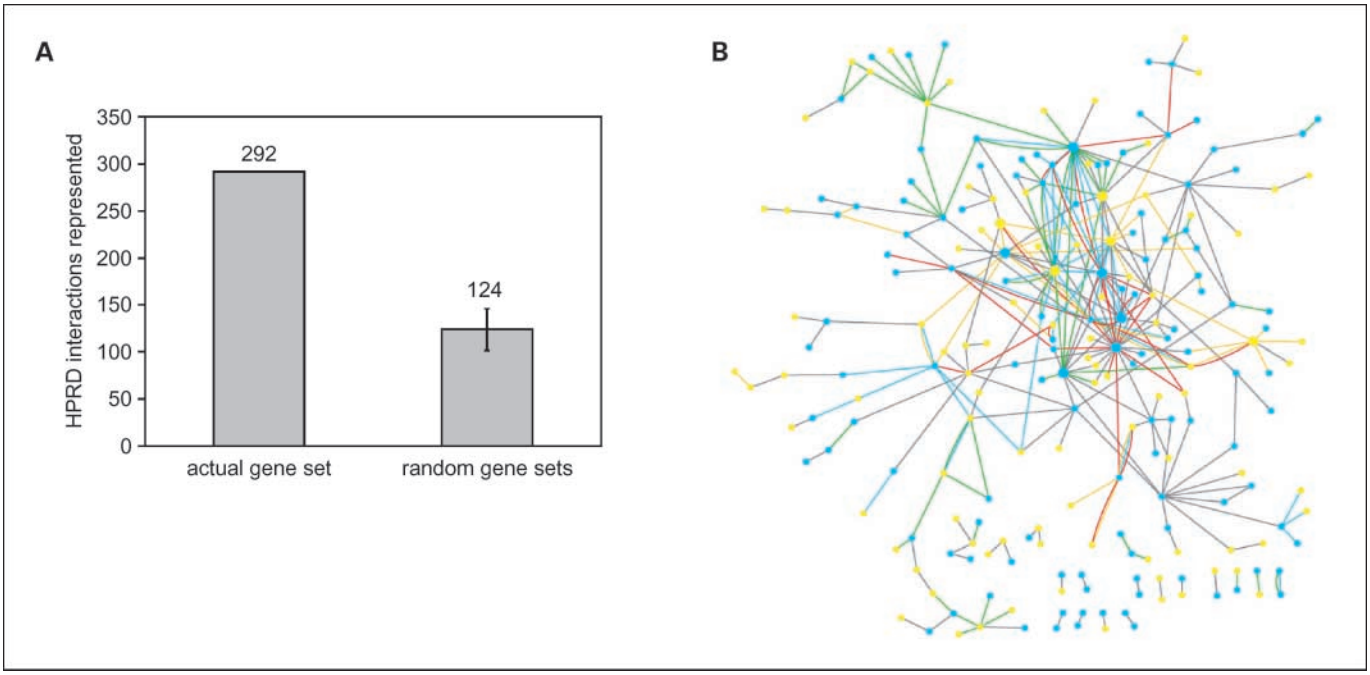

Fig. 3. Interaction network analysis of reactive stroma genes. *A,* number of known human protein-protein interactions (from Human Protein Reference Database) involving the 1,141 unique genes differentially expressed in reactive prostate stroma as compared with that expected from a random gene set of 1,141 (with ± 1 SD; based on 1,000 simulations). *B,* network representation of the entire set of 292 Human Protein Reference Database protein-protein interactions involving the 1,141 named genes differentially expressed in reactive prostate stroma. *C,* subnetwork of Human Protein Reference Database protein-protein interactions from (*B*). Nodes, genes; yellow nodes, genes overexpressed in reactive stroma; blue nodes, genes underexpressed in reactive stroma. A line between two nodes signifies that the corresponding protein products of the genes can physically interact (according to the literature). Colored edges (other than gray), a common gene ontology term annotation shared by both of the connected genes. Active hubs or genes connected to a significant number ($P < 0.01$; one-sided Fisher's exact test) of the other genes in the network appear enlarged over the other nodes.

that there are profound changes in cellular signaling in reactive stroma that may play a key role in the reactive stroma phenotype and may be targets for signal transduction inhibitors used for treatment of prostate cancer.

Up-regulated growth factor pathways in reactive stroma. To identify potential modulators of the profound changes seen in the reactive stroma, we identified growth factors, growth factor receptors, or growth factor receptor modulators that were up-regulated in reactive stroma ($P < 0.01$). These are shown in Table 3. Several major growth factor families are represented. Of note are the number of these proteins or protein families that have been linked to stem cell maintenance, including the Notch1, Kit, and the Wnt pathways. Other proteins such as ErbB2, fibroblast growth factor (FGF) 19, fibronectin leucine repeat transmembrane protein 1, endothelin receptor B, and glial cell–derived neurotrophic factor have been shown to be linked to neurogenesis, angiogenesis, and matrix remodeling. Some of these factors may also act as paracrine growth factors for prostate cancer cells. Wnt10b can bind Frizzled receptors, which are known to be expressed by prostate cancer cells (21). The glial cell–derived neurotrophic factor receptor RET is also known to be expressed in prostate cancer cells (22). Of course, Wnts and endothelins expressed by prostate cancer cells can also potentially act on the stromal cells. The endothelin 1 and TGF-β signaling pathway stimulation are important in up-regulation of collagen production and matrix remodeling (23). FGF19 specifically interacts with fibroblast growth factor receptor (FGFR-4), which is expressed in prostate cancer cells (24), but it requires the Klotho coreceptor to do so (25). Fibronectin leucine repeat transmembrane proteins have been shown to be up-regulated by FGF signaling and interact with FGFR-1 and are expressed at sites of FGF signaling in neural structures (26). Finally, the role of the TGF-β family is well established in prostate cancer stromal-epithelial interactions (4). Of note, it has been shown that increased expression of TGFBR2 in breast cancer stroma is associated with adverse outcome (27).

Alterations of reactive stroma matrix composition and proteins interacting with matrix. In addition to changes in cellular components, we also noted changes in cell matrix and matrix-interacting proteins in grade 3 reactive stroma. These are shown in Table 3. Cartilage oligomeric matrix protein is expressed in cartilage but can also be expressed in other sites and is known

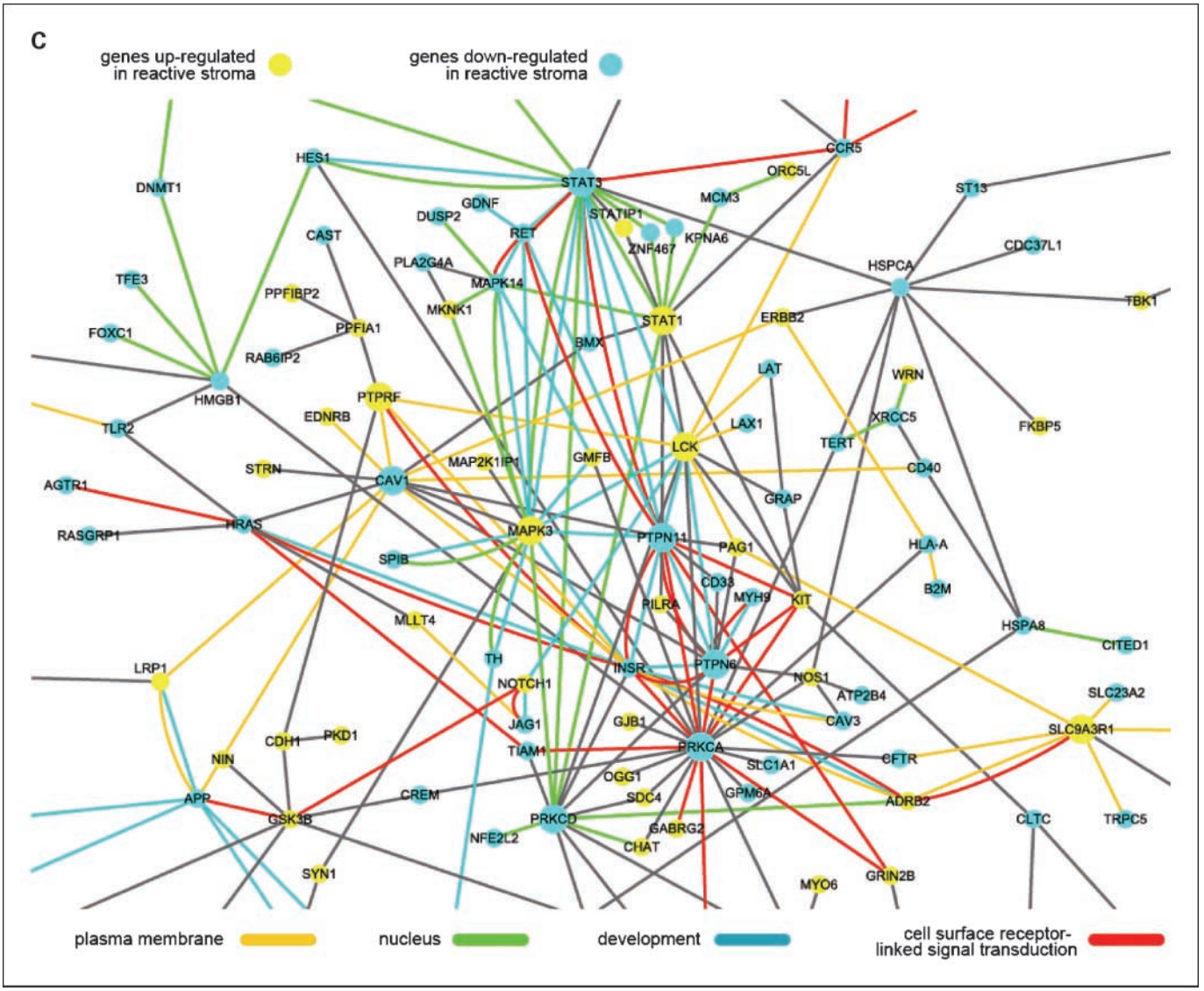

Table 3. Genes encoding growth factors, growth factor receptors, extracellular matrix proteins, and matrix-interacting proteins significantly up-regulated in reactive stroma ($P < 0.01$)

Growth factor families	Name	Symbol	P	Fold
EGF	v-erb-b2 Erythroblastic leukemia viral oncogene homolog 2	ERBB2	0.0046	1.7
FGF	FGF19	FGF19	0.0041	1.7
	Fibronectin leucine-rich transmembrane protein 1	FLRT1	0.0022	1.8
NOTCH	Notch homolog 1, translocation associated	NOTCH1	0.0078	1.7
WNT	Wingless-type MMTV integration site family, member 10B	WNT10b	0.0023	1.8
TGF-β	transforming growth factor, β receptor II	TGFBR2	0.0087	1.7
KIT	v-kit Feline sarcoma oncogene homolog	KIT	0.0067	1.7
Endothelin	Endothelin receptor type B	EDNRB	0.0058	1.7
Neurotrophin	Glial cell–derived neurotrophic factor	GDNF	0.0032	1.8
Extracellular matrix	Cartilage oligomeric matrix protein	COMP	0.0013	1.8
	Extracellular phosphoglycoprotein with ASARM motif	MEPE	0.0034	1.8
	Laminin α chain 2, merosin	LAMA2	0.0077	1.7
	Fibrinogen α chain	FGA	0.005	1.8
Matrix-interacting proteins	Syndecan 4	SDC4	0.000003	2.3
	Low-density lipoprotein–related protein 1	LRP1	0.0086	1.7
	Collagen type I and thrombospondin receptor	CD36	0.0001	2.1
	Thrombospondin 4	THBS4	0.0001	2.1

Abbreviation: EGF, epidermal growth factor.

to be up-regulated by TGF-β in prostatic stromal cells (28). It is known to be expressed by vascular smooth muscle cells and plays important role in adhesion and migration (29). MEPE has been linked to phosphate metabolism and plays a role in bone resorption and formation (30). MEPE is a member of the small integrin-binding ligand N-linked glycoprotein family gene family and are expressed in various cancers (31). Some of these proteins bind to and modulate matrix metalloprotease activity, but this has not been shown for MEPE to date. Laminin α 2 subunit is a component of laminin 2 and 4, which are expressed in peripheral nerve and neuromuscular junction, respectively (32). Laminin α 2 is a component of capillary vessels in the central nervous system (32), and interestingly, up-regulated expression of laminin α 2 may indicate changes in capillary basal membrane matrix favoring metastases in neuroendocrine carcinomas (33). Other proteins identified are well-known cellular proteins that interact with the extracellular matrix, such as CD36 (thrombospondin receptor, collagen type I receptor). Low-density lipoprotein–related protein 1 is a known receptor internalization factor enhancing TGF-β signaling, regulating extracellular matrix proteins such as fibronectin, matrix metalloprotease–9, and plasma membrane proteins such as urokinase-type plasminogen activator receptor (uPAR) and integrins (34, 35). It is a catabolic receptor for ECM structural proteins and for proteins that bind to ECM. Syndecan4 is involved in focal adhesion, cell spreading, integrin signaling, and stress fiber formation (36). Thrombospondin 4 is involved in neurite outgrowth, as well many other processes (37).

Gene expression changes in reactive stroma are associated with increased protein expression. To determine if increased mRNA levels in reactive stroma were associated with increased protein levels, we analyzed protein expression levels of extracellular signal-regulated kinase 1, c-KIT, and GSK-3β in normal and reactive stroma by immunohistochemistry using a small tissue microarray with 10 cancers with grade 3 reactive stroma and matched benign tissue. Typical results are shown in Supplementary Fig. 3. In all cases, increased protein expression was seen in the cancer stromal cells when compared with normal stroma.

Comparison of gene expression in prostate and breast cancer reactive stroma. Finak et al. (17) have recently reported the results of their gene expression microarray analysis of laser-captured breast cancer stroma from 53 primary breast cancers using method quite similar to ours. To identify similarities and differences between grade 3 reactive stroma from prostate cancer and breast cancer reactive stroma, we compared their expression data with our data set. A total of 75 transcript probes, representing 63 unique genes, were significantly up-regulated ($P < 0.01$; t test) in grade 3 prostate cancer and breast cancer reactive stroma when compared with their respective normal stromas. This overlap had a borderline statistical significance ($P < 0.02$; one-sided Fisher's exact test). The expression patterns of the 776 probes up-regulated in grade 3 reactive prostate cancer stroma in the breast cancer stroma and normal breast stroma are shown in Fig. 4 (along with the average expression for the entire gene set). Overall, the grade 3 prostate cancer up-regulated stromal genes were increased in breast cancer stroma compared with normal breast stroma, but many individual genes were decreased. Furthermore, the overlap between the down-regulated genes was not statistically significant ($P = 0.30$). Thus, there were some similarities between prostate cancer stroma and breast cancer stroma, but there were differences as well. A gene ontology analysis of the commonly up-regulated genes found seven of the nine top enriched gene ontology terms ($P < 0.001$) being related directly or indirectly to DNA damage response and two being related to caspase regulation (Supplementary Table S4).

Discussion

During prostate cancer progression, stromal reaction occurs resulting in development of a reactive stroma microenvironment that is different from normal prostate stroma. Here, we have analyzed expression changes taking place in grade 3

reactive stroma, which has been shown to be associated with prostate cancer progression. A total of 1,141 genes were differentially expressed in reactive stroma (at $P < 0.01$), which was significantly higher than would be expected by chance alone and indicates that there are profound changes in gene expression associated with formation of reactive stroma in prostate cancer. This is presumably due to changes in the types of cells present and changes in gene expression of individual cells. Gene ontology analysis reveals significant functional clustering of these genes. Of particular interest is a significant increase in the level of expression for genes responsible for neurogenesis, axonogenesis, synaptogenesis, and neural biogenesis, indicating that active neurogenesis and axonogenesis is occurring in grade 3 reactive stroma. We observed an increased expression of several genes involved in neural development, such as *GDNF*, *NOTCH1*, *FGF19*, *GLI2*, and *CDK5*. The glial cell–derived neurotrophic factor is neurotrophic stem cell factor, promoting survival and differentiation of neurons and preventing an apoptosis of motor neurons induced by axotomy. In some neural processes, glial cell–derived neurotrophic factor can increase cyclin-dependent kinase 5 activity (38, 39). Cyclin-dependent kinase 5 is a well-known kinase involved in neuronal migration and guidance. Another up-regulated neural development factor, GLI2, is a well-known zinc-finger protein of the GLI family. It is a transcriptional mediator of Shh signaling, involved in patterning of dorsal-ventral axis of the spinal cord. It has been shown that TGF-β induces expression of GLI2 in many type of cells, including fibroblasts and LNCaP prostate cancer cells (40). We have shown previously significant biological interactions of nerves and cancer cells in prostate cancer (41, 42), and our findings indicate that not only do cancer cells interact with pre-existing nerves but also they may actually induce formation of nerves *in vivo*. Recent data from our group have shown the occurrence of axonogenesis and neurogenesis in prostate cancer by quantitative analysis nerves and neurons in prostate cancer and normal controls (43). Of note, our *in vitro* studies have identified semaphorin 4F as a key factor in prostate cancer–induced neurogenesis, and our current data show that semaphorin 4F is significantly up-regulated in prostate cancer reactive stroma *in vivo*. Other molecules identified in analysis may also play important roles the complex process of axonogenesis and neurogenesis.

Another novel observation is the prominence of the DNA damage signaling pathway in reactive stroma. Our results show up-regulated expression of *MRE11A*, a member of Mre11-Nbs1-Rad50 complex responsible for DNA double strand–break repair (44). At the same time, we found an increased expression of 9-1-1 complex members *HUS1* and *RAD17*, which are both involved in cellular response to many types of DNA damage and participate in DNA replication fork stabilization, G_2/M arrest, and DNA repair (45). The reason for the DNA damage response observed in reactive stroma is not clear but may be due to reactive oxygen species generated within the stroma, perhaps by inflammatory cells or by the cancer cells (46).

A potential important finding is the enrichment for terms related to somatic stem cells. There has been increasing evidence in recent years that somatic stem cells may play a role in generation of reactive stroma. This term was not identified in our gene ontology analysis because only a few genes have been identified that are critical in stem cell biology, and thus, 10 genes were not present on our array. Among the up-regulated factors we identified was *BMI-1*, which is well known as a gene that is expressed in stem cells from various tissues and plays an important role in their maintenance (47). *NOTCH1* is also up-regulated in reactive stroma and plays an

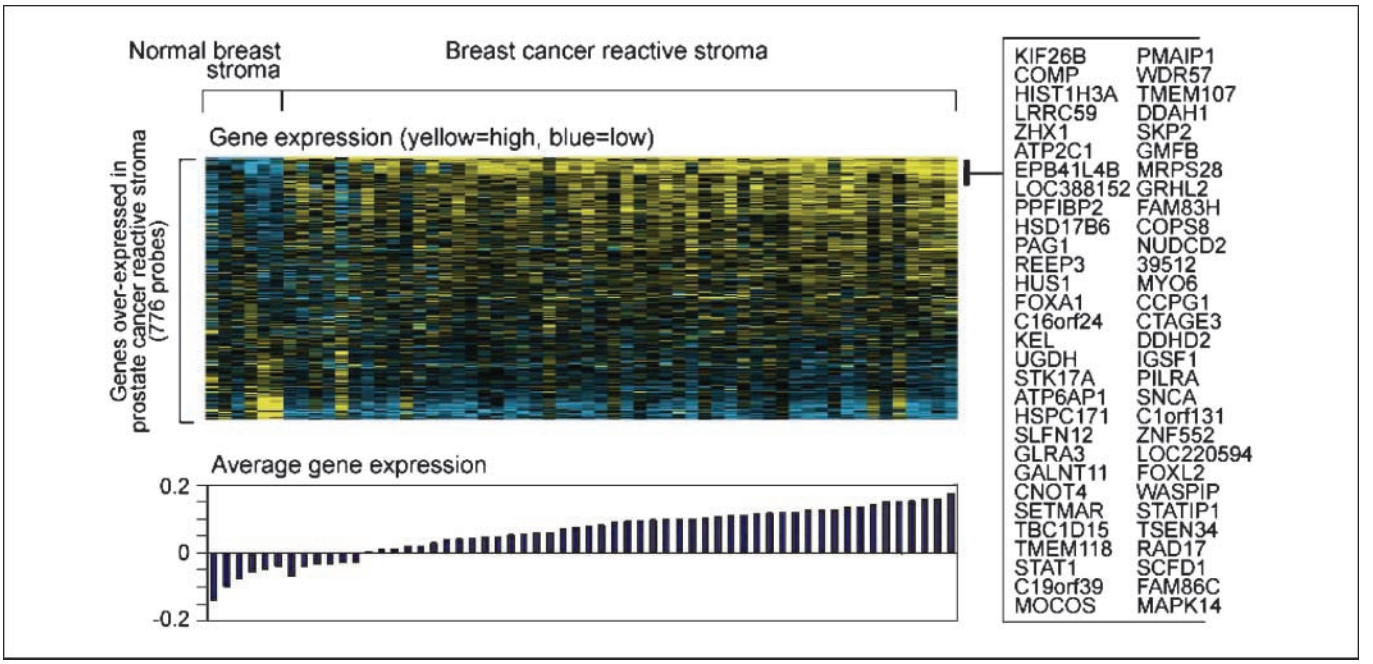

Fig. 4. Expression patterns in breast cancer reactive stroma for genes overexpressed in prostate cancer reactive stroma. Referring to the profiling data set from Finak et al. (15) of normal breast stroma ($n = 6$) and breast cancer reactive stroma ($n = 52$), the 776 transcript probes that are in that data set and showing overexpression in grade 3 prostate cancer reactive stroma (Fig. 2A) were examined. Top, gene expression heat map (genes ordered from high to low expression in reactive stroma). Bottom, average expression of the (mean centroid, centered) genes for the corresponding sample profiles. Unique genes (those with a common name) showing overexpression in both prostate and breast reactive stroma in indicated region ($P < 0.01$ each data set) are listed.

important role stem cell self-renewal (48). In addition, *C-KIT* and components of the Wnt pathway are also up-regulated and have been shown to be involved in stem cell proliferation (49, 50). A recent report by Mishra et al. (51) has shown that human mesenchymal stem cells can be induced *in vitro* by tumor-conditioned media to differentiate into myofibroblast cells, typically observed in tumor-associated reactive stroma. It is of particular interest that gene expression analysis of mesenchymal stem cells treated with tumor cell–conditioned medium showed elevated expression of several neurogenesis/axonogenesis-related genes that we have shown to be up-regulated in reactive stroma *in vivo*, including *CDK5* and *Semaphorin 4F*, which were linked to the axon guidance pathway by these authors. These *in vitro* studies imply that mesenchymal stem cells may give rise to neural cells, as well as myofibroblastic cells in prostate cancer reactive stroma. As discussed by Mishra et al. (51), the origin of mesenchymal stem cells in tumor reactive is not completely established, but at least, a subset is derived from circulating marrow cells.

To date, there have only been limited studies on gene expression in prostatic stroma and even fewer of reactive stroma in prostate cancer. To our knowledge, the only direct comparison of normal and reactive stroma in prostate cancer is the study by Richardson et al. (52) of five cases using laser-captured normal and tumor-associated stroma. A total of 44 genes were consistently up-regulated in all five cases in the tumor stroma. Although their analytic approach was quite different than ours, we still noted overlap of their 44-gene set and our 544 up-regulated genes, including *FOXA1*, *COMP*, *STEAP1*, and *CPNE4*. This group also found increases of *FOLH1* (*PSMA*). This gene is expressed in prostate cancer tumor vasculature (53), and we also found this gene to be increased, although it was slightly outside our statistical cutoff ($P = 0.011$). It should be noted that their study used unselected prostate cancer cases, whereas we focused on grade 3 reactive stroma. We are currently assessing gene expression changes in grade 1 and 2 reactive stroma to identify the key components in the grade 3 stroma that may be enhancing prostate cancer progression.

Our comparison of breast cancer stroma to prostate cancer grade 3 reactive stroma reveals a partial overlap of gene expression signatures in these two tissues. It is not surprising that there are significant differences in the reactive stroma between these two cancers given the very significant differences in the biology of these cancers and the fact that the normal prostate stroma is predominantly smooth muscle whereas breast stroma is predominantly fibrous and adipose tissue. However, the finding that the DNA damage pathway is also up-regulated in breast cancer stroma supports our finding that this pathway is increased in prostate cancer stroma. As noted above, mutations of p53 have been identified in breast cancer stroma (19), consistent with the occurrence of DNA damage. In particular, increased expression of *HUS1* and *RAD17* was seen in stroma of both cancer types. Interestingly, both *FOXA1* and *COMP* were increased in breast cancer stroma and in prostate cancer stroma, in our data set and that of Richardson et al. (52), supporting their role in reactive stroma biology. Thus, there are significant similarities, as well as differences, in reactive stroma from these two cancer sites. Of note, we did not find a statistically significant overlap of our gene set with the "wound healing" gene expression signature derived from serum-stimulated fibroblasts, as defined by Chang et al. (54), that has been shown to have prognostic significance for a number of cancers, including breast cancer, when nonmicrodissected tissues are analyzed (data not shown). This is not completely surprising because many of the genes that are components of this signature are expressed predominantly in cancer epithelial cell when analyzed by immunohistochemistry or *in situ* hybridization (54). Further studies in various common cancer types may identify common and tissue type–specific pathways activated and repressed in cancer stroma.

In summary, our studies indicate that formation of prostate cancer reactive stroma is a complex dynamic process involving a number of growth factor pathways and characterized by activation of multiple processes, including neurogenesis and axonogenesis. Further studies are needed to identify the key individual biomarkers of progression in grade 3 reactive stroma. In addition, we have identified potential therapeutic targets in prostate cancer stroma and key signal transduction pathways that may be useful in treatment of patients with aggressive prostate cancer.

Disclosure of Potential Conflicts of Interest

No potential conflicts of interest were disclosed.

Acknowledgments

We thank Deanna Killen and Shantu Dixit for the technical assistance.

References

1. Tuxhorn JA, Ayala GE, Rowley DR. Reactive stroma in prostate cancer progression. J Urol 2001;166:2472–83.
2. Chung LW, Baseman A, Assikis V, Zhau HE. Molecular insights into prostate cancer progression: the missing link of tumor microenvironment. J Urol 2005;173:10–20.
3. Alberti C. Prostate cancer progression and surrounding microenvironment. Int J Biol Markers 2006;21:88–95.
4. Tuxhorn JA, Ayala GE, Smith MJ, Smith VC, Dang TD, Rowley DR. Reactive stroma in human prostate cancer: induction of myofibroblast phenotype and extracellular matrix remodeling. Clin Cancer Res 2002;8:2912–23.
5. Tuxhorn JA, McAlhany SJ, Dang TD, Ayala GE, Rowley DR. Stromal cells promote angiogenesis and growth of human prostate tumors in a differential reactive stroma (DRS) xenograft model. Cancer Res 2002;62:3298–307.
6. Ayala G, Tuxhorn JA, Wheeler TM, et al. Reactive stroma as a predictor of biochemical-free recurrence in prostate cancer. Clin Cancer Res 2003;9:4792–801.
7. Yanagisawa N, Rowley D, Kadmon D, Miles BJ, Wheeler TM, Ayala GE. Stromogenic prostatic carcinoma pattern (carcinomas with reactive stromal grade 3) in needle biopsies predicts biochemical recurrence-free survival in patients after radical prostatectomy. Hum Pathol 2008;39:282–91.
8. Gentleman R, Carey V, Huber W, Irizarry R, Dudoit S. Bioinformatics and computational biology solutions using R and Bioconductor. Springer Science+Business Media, Inc.; New York. 2005.
9. Johnson W, Li C, Rabinovic A. Adjusting batch effects in microarray expression data using Empirical Bayes methods. Biostatistics 2007;8:118–27.
10. Storey JD, Tibshirani R. Statistical significance for genomewide studies. Proc Natl Acad Sci U S A 2003;100:9440–5.
11. Eisen MB, Spellman PT, Brown PO, Botstein D. Cluster analysis and display of genome-wide expression patterns. Proc Natl Acad Sci U S A 1998;95:14863–8.
12. Saldanha AJ. Java Treeview-extensible visualization of microarray data. Bioinformatics 2004;20:3246–8.
13. Creighton C, Kuick R, Misek DE, et al. Profiling of pathway-specific changes in gene expression following growth of human cancer cell lines transplanted into mice. Genome Biol 2003;4:R46.
14. Creighton CJ, Bromberg-White JL, Misek DE, et al. Analysis of tumor-host interactions by gene expression profiling of lung adenocarcinoma xenografts

identifies genes involved in tumor formation. Mol Cancer Res 2005;3:119–29.
15. Shannon P, Markiel A, Ozier O, et al.Cytoscape: a software environment for integrated models of biomolecular interaction networks. Genome Res 2003; 13:2498–504.
16. Cai Y, Wang J, Li R, Ayala G, Ittmann M, Liu M. GGAP2/PIKE-a directly activates both the Akt and nuclear factor-kappaB pathways and promotes prostate cancer progression. Cancer Res 2009;69:819–27.
17. Finak G, Bertos N, Pepin F, Sadekova S, et al. Stromal gene expression predicts clinical outcome in breast cancer. Nat Med 2008;14:518–27.
18. Zhu B, Xu F, Baba Y. An evaluation of linear RNA amplification in cDNA microarray gene expression analysis. Mol Genet Metab 2006;87:71–9.
19. Patocs A, Zhang L, Xu Y, et al. Breast-cancer stromal cells with TP53 mutations and nodal metastases. N Engl J Med 2007;357:2543–51.
20. Peri S, Navarro J, Amanchy R, et al. Development of human protein reference database as an initial platform for approaching systems biology in humans. Genome Res 2003;13:2363–71.
21. Joesting MS, Perrin S, Elenbaas B, et al. Identification of SFRP1 as a candidate mediator of stromal-to-epithelial signaling in prostate cancer. Cancer Res 2005;65:10423–30.
22. Dawson DM, Lawrence EG,MacLennan GT, et al. Altered expression of *RET* proto-oncogene product in prostatic intraepithelial neoplasia and prostate cancer. J Natl Cancer Inst 1998;90:519–23.
23. Horstmeyer A, Licht C, Scherr G, Eckes B, Krieg T. Signalling and regulation of collagen I synthesis by ET-1 and TGF-beta1. FEBS J 2005;272:6297–309.
24. Wang J, Stockton DW, Ittmann M. The fibroblast growth factor receptor-4 *Arg388* allele is associated with prostate cancer initiation and progression. Clin Cancer Res 2004;10:6169–78.
25. Kurosu H, Choi M, Ogawa Y, et al. Tissue-specific expression of betaKlotho and fibroblast growth factor (FGF) receptor isoforms determines metabolic activity of FGF19 and FGF21. J Biol Chem 2007;282: 26687–95.
26. Haines BP, Wheldon LM, Summerbell D, Heath JK, Rigby PW. Regulated expression of *FLRT* genes implies a functional role in the regulation of FGF signalling during mouse development. Dev Biol 2006; 297:14–25.
27. Barlow J, Yandell D, Weaver D, Casey T, Plaut K. Higher stromal expression of transforming growth factor-beta type II receptors is associated with poorer prognosis breast tumors. Breast Cancer Res Treat 2003;79:149–59.
28. Untergasser G, Gander R, Lilg C, Lepperdinger G, Plas E, Berger P. Profiling molecular targets of TGF-beta1 in prostate fibroblast-to-myofibroblast transdifferentiation. Mech Ageing Dev 2005;126: 59–69.
29. Riessen R, Fenchel M, Chen H, Axel DI, Karsch KR, Lawler J. Cartilage oligomeric matrix protein (thrombospondin-5) is expressed by human vascular smooth muscle cells. Arterioscler Thromb Vasc Biol 2001;21:47–54.
30. White KE, Larsson TE, Econs MJ. The roles of specific genes implicated as circulating factors involved in normal and disordered phosphate homeostasis: frizzled related protein-4, matrix extracellular phosphoglycoprotein, and fibroblast growth factor 23. Endocr Rev 2006;27:221–41.
31. Fisher LW, Jain A, Tayback M, Fedarko NS. Small integrin binding ligand N-linked glycoprotein gene family expression in different cancers. Clin Cancer Res 2004;10:8501–11.
32. Vitolo D, Ciocci L, Cicerone E, et al. Laminin alpha2 chain (merosin M chain) distribution and *VEGF, FGF(2)*, and *TGFbeta1* gene expression in angiogenesis of supraglottic, lung, and breast carcinomas. J Pathol 2001;195:197–208.
33. Vitolo D, Ciocci L, Deriu G, et al. Laminin alpha2 chain-positive vessels and epidermal growth factor in lung neuroendocrine carcinoma: a model of a novel cooperative role of laminin-2 and epidermal growth factor in vessel neoplastic invasion and metastasis. Am J Pathol 2006;168:991–1003.
34. Cabello-Verrugio C, Brandan E. A novel modulatory mechanism of transforming growth factor-beta signaling through decorin and LRP-1. J Biol Chem 2007; 282:18842–50.
35. Gaultier A, Salicioni AM, Arandjelovic S, Gonias SL. Regulation of the composition of the extracellular matrix by low density lipoprotein receptor-related protein-1: activities based on regulation of mRNA expression. J Biol Chem 2006;281:7332–40.
36. Rapraeger AC. Molecular interactions of syndecans during development. Semin Cell Dev Biol 2001;12: 107–16.
37. Arber S, Caroni P. Thrombospondin-4, an extracellular matrix protein expressed in the developing and adult nervous system promotes neurite outgrowth. J Cell Biol 1995;131:1083–94.
38. Airaksinen MS, Saarma M. The GDNF family: signalling, biological functions and therapeutic value. Nat Rev Neurosci 2002;3:383–94.
39. Ledda F, Paratcha G, Ibanez CF. Target-derived GFRalpha1 as an attractive guidance signal for developing sensory and sympathetic axons via activation of Cdk5. Neuron 2002;36:387–401.
40. Dennler S, Andre J, Alexaki I, et al. Induction of sonic hedgehog mediators by transforming growth factor-beta: Smad3-dependent activation of Gli2 and Gli1 expression *in vitro* and *in vivo*. Cancer Res 2007;67:6981–6.
41. Ayala GE, Wheeler TM, Shine HD, et al. *In vitro* dorsal root ganglia and human prostate cell line interaction: redefining perineural invasion in prostate cancer. Prostate 2001;49:213–23.
42. Ayala GE, Dai H, Tahir SA, et al. Stromal antiapoptotic paracrine loop in perineural invasion of prostatic carcinoma. Cancer Res 2006;66:5159–64.
43. Ayala GE, Dai H, Powell M, et al. Cancer related axonogenesis and neurogenesis in prostate cancer. Clin Cancer Res. In Press 2008.
44. Lavin MF. ATM and the Mre11 complex combine to recognize and signal DNA double-strand breaks. Oncogene 2007;26:7749–58.
45. Parrilla-Castellar ER, Arlander SJ, Karnitz L. Dial 9-1-1 for DNA damage: the Rad9-1-Rad1 (9-1-1) clamp complex. DNA Repair (Amst) 2004;3:1009–14.
46. Kumar B, Koul S, Khandrika L, Meacham RB, Koul HK. Oxidative stress is inherent in prostate cancer cells and is required for aggressive phenotype. Cancer Res 2008;68:1777–85.
47. Glinsky GV. "Stemness" genomics law governs clinical behavior of human cancer: implications for decision making in disease management. J Clin Oncol 2008;26:2846–53.
48. Fox V, Gokhale PJ, Walsh JR, Matin M, Jones M, Andrews PW. Cell-cell signaling through NOTCH regulates human embryonic stem cell proliferation. Stem Cells 2008;26:715–23.
49. Bashamboo A, Taylor AH, Samuel K, Panthier JJ, Whetton AD, Forrester LM. The survival of differentiating embryonic stem cells is dependent on the SCF-KIT pathway. J Cell Sci 2006;119:3039–46.
50. Nemeth MJm, Topol L, Anderson SM, Yang Y, Bodine DM. Wnt5a inhibits canonical Wnt signaling in hematopoietic stem cells and enhances repopulation. Proc Natl Acad Sci U S A 2007;104: 15436–41.
51. Mishra PJ, Humeniuk R, Medina DJ, et al. Carcinoma-associated fibroblast-like differentiation of human mesenchymal stem cells. Cancer Res 2008;68: 4331–9.
52. Richardson AM, Woodson K, Wang Y, et al. Global expression analysis of prostate cancer-associated stroma and epithelia. Diagn Mol Pathol 2007;16: 189–97.
53. Chang SS, Reuter VE, Heston WD, Bander NH, Grauer LS, Gaudin PB. Five different anti-prostate-specific membrane antigen (PSMA) antibodies confirm PSMA expression in tumor-associated neovasculature. Cancer Res 1999;59:3192–8.
54. Chang HY, Sneddon JB, Alizadeh AA, et al. PLoS Biol;2:E7.

Clinical Cancer Research

Global Gene Expression Analysis of Reactive Stroma in Prostate Cancer

Olga Dakhova, Mustafa Ozen, Chad J. Creighton, et al.

Clin Cancer Res 2009;15:3979-3989.